Biochemistry and Biophysics Reports 42 (2025) 102012

Contents lists available at ScienceDirect

Biochemistry and Biophysics Reports

journal homepage: www.elsevier.com/locate/bbrep

Dynamic changes of intracellular signals in ATTR Tyr114Cys amyloidosis

Kenta Ouchi [a], Takeshi Masuda [b], Kou Yonemaru [a], Kaori Isono [c], Yuki Ohya [c,d], Nobuaki Shiraki [e], Masayoshi Tasaki [f,g], Yukihiro Inomata [d], Mitsuharu Ueda [g], Takumi Era [h], Shoen Kume [e], Yukio Ando [i], Hirofumi Jono [a,j,*]

[a] Department of Clinical Pharmaceutical Sciences, Graduate School of Pharmaceutical Sciences, Kumamoto University, 2-2-1 Honjo, Chuo Ward, Kumamoto City, Kumamoto Prefecture, 860-8556, Japan
[b] Graduate School of Media and Governance / Institute for Advanced Biosciences, Keio University, 14-1 Baba-machi, Tsuruoka-City, Yamagata Prefecture, 997-0035, Japan
[c] Department of Transplantation and Paediatric Surgery, Graduate School of Medical Science, Kumamoto University, 1-1-1 Honjo, Chuo Ward, Kumamoto City, Kumamoto Prefecture, 860-8556, Japan
[d] Department of Pediatric Surgery, Kumamoto Rosai Hospital, 1670 Takehara-cho, Yatsushiro City, Kumamoto Prefecture, 866-0826, Japan
[e] School of Life Science and Technology, Tokyo Institute of Technology, 4259 Nagatsuta-cho, Midori Ward, Yokohama City, Kanagawa Prefecture, 226-8501, Japan
[f] Department of Biomedical Laboratory Sciences, Graduate School of Health Sciences, Kumamoto University, Kumamoto, 1-1-1 Honjo, Chuo Ward, Kumamoto City, Kumamoto Prefecture, 860-8556, Japan
[g] Department of Neurology, Graduate School of Medical Science, Kumamoto University, 1-1-1 Honjo, Chuo Ward, Kumamoto City, Kumamoto Prefecture, 860-8556, Japan
[h] Department of Cell Modulation, Institute of Molecular Embryology and Genetics, Kumamoto University, 2-2-1 Honjo, Chuo Ward, Kumamoto City, Kumamoto Prefecture, 860-8556, Japan
[i] Department of Amyloidosis Research, Nagasaki International University, 2825-7 Huis Ten Bosch Cho, Sasebo City, Nagasaki Prefecture, 859-3298, Japan
[j] Department of Pharmacy, Kumamoto University Hospital, 1-1-1 Honjo, Chuo Ward, Kumamoto City, Kumamoto Prefecture, 860-8556, Japan

ARTICLE INFO

Keywords:
ATTR amyloidosis
Transthyretin
Induced pluripotent stem cells
Proteomic analysis

ABSTRACT

Hereditary transthyretin (TTR) amyloidosis (ATTRv amyloidosis) is an autosomal dominant disease caused by various TTR mutations. Despite the fact that ATTR Tyr114Cys (p.Tyr134Cys) amyloidosis (tyrosine to cysteine at codon 114) exhibits poorer prognosis than other ATTRv amyloidosis and leads to death due to severe clinical symptoms, the molecular pathogenesis of ATTR Tyr114Cys amyloidosis is still largely unknown. In this study, we took advantage of ATTR Tyr114Cys amyloidosis-specific induced pluripotent stem (iPS) cells to differentiate into hepatocyte-like cells (Y114C-HLCs), which are mainly TTR producing cells, and elucidated their pathogenesis. We performed proteomic analysis to comprehensively identify specific intracellular signaling pathways involved in Y114C-HLCs, and identified the specific proteins changed only in Y114C-HLCs, in comparison with disease control HLCs from ATTR Val30Met amyloidosis (V30M-HLCs). Moreover, we have succeeded in identifying several specific intracellular signals that are significantly activated in Y114C-HLCs, including cellular responses to stress and extracellular matrix organization. Our proteomic analysis is the first to report that the specific point mutations in ATTRv amyloidosis cause dynamic changes in cellular response, and reveal the specific intracellular signals may be involved in the specific pathogenesis of ATTR Tyr114Cys amyloidosis.

1. Introduction

Hereditary transthyretin (TTR) amyloidosis (ATTRv amyloidosis) is an autosomal dominant disease caused by variant TTR mutation, with a poor prognosis about 10 years of life expectancy [1]. Amyloidogenic TTR (ATTR) by TTR gene mutation, is mainly synthesized by liver & circulates in the blood, and causes amyloid fibrils deposition, which in turn, leads to various symptoms [2]. In association with the fact that more than 150 different point mutations have been identified, ATTRv amyloidosis exhibits several different phenotypes, such as peripheral neuropathy, heart failure and central nervous system (CNS) symptoms, due to its specific TTR mutation [3].

* Corresponding author. Department of Clinical Pharmaceutical Sciences, Graduate School of Pharmaceutical Sciences, Kumamoto University, 2-2-1 Honjo, Chuo Ward, Kumamoto City, Kumamoto Prefecture, 860-8556, Japan.
E-mail address: hjono@kuh.kumamoto-u.ac.jp (H. Jono).

https://doi.org/10.1016/j.bbrep.2025.102012
Received 25 October 2024; Received in revised form 4 April 2025; Accepted 7 April 2025

Among various types of ATTRv amyloidosis, ATTR Tyr114Cys (p.Tyr134Cys) amyloidosis (tyrosine to cysteine at codon 114) exhibits poorer prognosis than other ATTRv amyloidosis by severe clinical symptoms resulting in death [4,5]. ATTR Tyr114Cys shows cerebral amyloid angiopathy by ATTR amyloid deposition in the meningeal & brain blood vessel walls, which may cause fatal cerebral haemorrhage and CNS symptoms, such as cognitive decline and cramps [5]. In contrast, ATTR Val30Met (p.Val50Met) amyloidosis (valine to methionine at codon 30), a representative peripheral neuropathy type, is caused by systemic ATTR amyloid depositions in various organs by liver derived ATTR [6]. Although there is clinically-effective treatment targeting ATTR derived from liver based on the pathogenesis of ATTR Val30Met amyloidosis focusing on TTR synthesis process [6–8], no treatment is available for ATTR Tyr114Cys amyloidosis due to unknown molecular pathogenesis.

Induced pluripotent stem (iPS) cells have pluripotency that can differentiate into most cell types [9–11]. Particularly, disease-specific iPS cells, generated from patients with hereditary diseases, can be useful pathological models maintaining patient's genetic information, by taking advantage of the pluripotency of iPS cells. Our previous report has shown that hepatocyte-like cells (HLCs) differentiated from ATTR Tyr114Cys amyloidosis-specific iPS cells (Y114C-iPS cells), exhibited the clinical phenotype of ATTR Tyr114Cys amyloidosis [12,13]. Consistent with clinical evidence that blood ATTR levels in ATTR Tyr114Cys amyloidosis was less than ATTR Val30Met amyloidosis [12], HLCs differentiated from Y114C-iPS cells (Y114C-HLCs) indeed exhibited low ATTR-Y114C secretion. Those results revealed that Y114C-HLCs could be useful tool to elucidate the molecular pathogenesis, also strongly suggesting that the specific mutation (only one amino acid replacement in this case) made a significant difference in cellular processes of HLCs. However, the molecular mechanism underlying the different clinical phenotypes focusing on TTR synthesis process, due to its specific TTR mutation, has yet to be determined.

In this study, we took advantage of ATTRv amyloidosis-specific iPS cells, and performed proteome analysis to comprehensively identify intracellular signalling pathways involved in TTR synthesis process in Y114C-HLCs, for elucidating the molecular pathogenesis of ATTR Tyr114Cys amyloidosis.

2. Materials & methods

2.1. iPS cell lines and differentiation into hepatocyte-like cells (HLCs)

ATTRv amyloidosis-specific iPS cells (Y114C-iPS cells and V30M-iPS cells) and 201B7 cells (WT-iPS cells) as control [10,13,14] were used. Methods for establishing iPS cell lines and differentiating into HLCs using feeder free method protocol have been described previously [13,14]. Briefly, we first used activin A to differentiate into definitive endoderm cells from iPS cells. And then, hepatocyte growth factor and Oncostatin M was treated to differentiate the definitive endoderm cells into hepatocytes. We investigated HLCs differentiated from each iPS cell lines (WT-HLCs, Y114C-HLCs and V30M-HLCs). This study was approved by the Research Ethics Committee of Kumamoto University Hospital (approved number: No. 981), and conducted after obtaining written informed consent.

2.2. Proteomic analysis

The whole cell lysate of HLCs was prepared by phase transfer surfactant (PTS) method as described previously [15,16]. Sodium deoxycholate (SDC), sodium N-lauroylsarcosinate (SLS), ammonium bicarbonate, dithiothreitol (DTT), iodoacetamide (IAA), mass spectrometry grade lysyl endoprotease (Lys-C), ethyl acetate, acetonitrile, acetic acid, and trifluoroacetic acid (TFA) were purchased from FUJIFILM Wako Pure Chemical Corporation (Osaka, Japan). Modified trypsin was from Promega (Madison, MA). 4-(2-Aminoethyl) benzenesulfonyl fluoride hydrochloride was from Nacalai (Kyoto, Japan).

Proteins were extracted with PTS solution (12 mM SDC, 12 mM SLS, and 50 mM ammonium bicarbonate containing 1 mM 4-(2-aminoethyl) benzenesulfonyl fluoride hydrochloride) and ultrasonic crushing for 20 min. After incubating for 5 min at 95 °C, proteins in the supernatant solution were quantified by the BCA method using a Pierce BCA Protein Assay Kit.

Proteins were reduced with 10 mM DTT for 30 min at room temperature and alkylated with 50 mM IAA in the dark for 30 min at room temperature. The protein mixture was 5-folds diluted with 50 mM ammonium bicarbonate. And then, mixture was digested with Lys-C (1/20 sample weight) at room temperature for 3 h prior to the addition of trypsin (1/20 sample weight) and incubation at 37 °C overnight. An equal volume of ethyl acetate was added to the eluent solution, and the mixture was acidified with 0.5 % TFA (final concentration). The mixture was shaken for 2 min and centrifuged at 15,600×*g* for 2 min at room temperature. After remove the solution in a vacuum evaporator, suspension the sample in 100 μL buffer A (5 % acetonitrile, 0.1 % TFA) and desalt with GL-Tip SDB (GL Science, Tokyo, Japan) [17,18]. Peptides were eluted in buffer B (80 % acetonitrile, 0.1 % TFA).

Orbitrap Exploris 480 (Thermo Fisher Scientific, Carlsbad, CA, USA) equipped with a Vanquish NEO UHPLC system (Thermo Fisher Scientific) was employes for nanoLC-MS/MS measurement. The injection volume was 5 μL, and the flow rate was 300 nL/min. An analytical column (3 μm, 75 μm ID, 12 cm length, Nikkyo Technols, Tokyo, Japan) were used. For peptide identification, data were acquired in the data-independent acquisition mode and analyzed using DIA-NN 1.8 with the UniProt human reference proteome database allowing one miss-cleavage [19]. The protein identification and quantification confidence for the dataset was evaluated on the basis of the FDR. For phosphoproteomics, data were acquired in the data-dependent acquisition mode and analyzed using MaxQuant v.2.4.9.0 with the dynamic modification of phosphorylation on serine, threonine, and tyrosine [20].

The MS data files have been deposited in the ProteomeXchange Consortium (http://www.proteomexchange.org/, PXD047155) via the jPOST partner repository (https://jpostdb.org, JPST002398) [21].

2.3. Statistical analysis

We used *t*-test to evaluate the difference (2-folds change) between Y114C-HLCs and WT-HLCs, or between V30M-HLCs and WT-HLCs, respectively (n = 3, independently). Statistical significance was defined as $p < 0.05$.

2.4. Bioinformatics analysis

Gene ontology (GO) analysis was performed by Metascape, a web-based portal which provides comprehensive gene annotation based on GO processes, Reactome gene set [22]. We used the proteins that have significantly altered expression levels Y114C-HLCs and V30M-HLCs, respectively, comparison to WT-HLCs. Based on the proteins identified by GO analysis, we further performed Reactome pathway analysis to elucidate the specific intracellular signals [23].

3. Results

3.1. Proteome analysis of Y114C-HLCs

To elucidate the molecular pathogenesis of ATTR Tyr114Cys amyloidosis, we first performed proteomic analysis to comprehensively identify the specific intracellular signaling pathway involved in HLCs differentiated from Y114C cells (Y114C-HLCs). Proteomic analysis detected approximately 7000 proteins in Y114C-HLCs, as well as HLCs differentiated from WT-iPS cells (WT-HLCs) and from V30M-iPS cells (V30M-HLCs) (Fig. 1A). In comparison with WT-HLCs, volcano plots

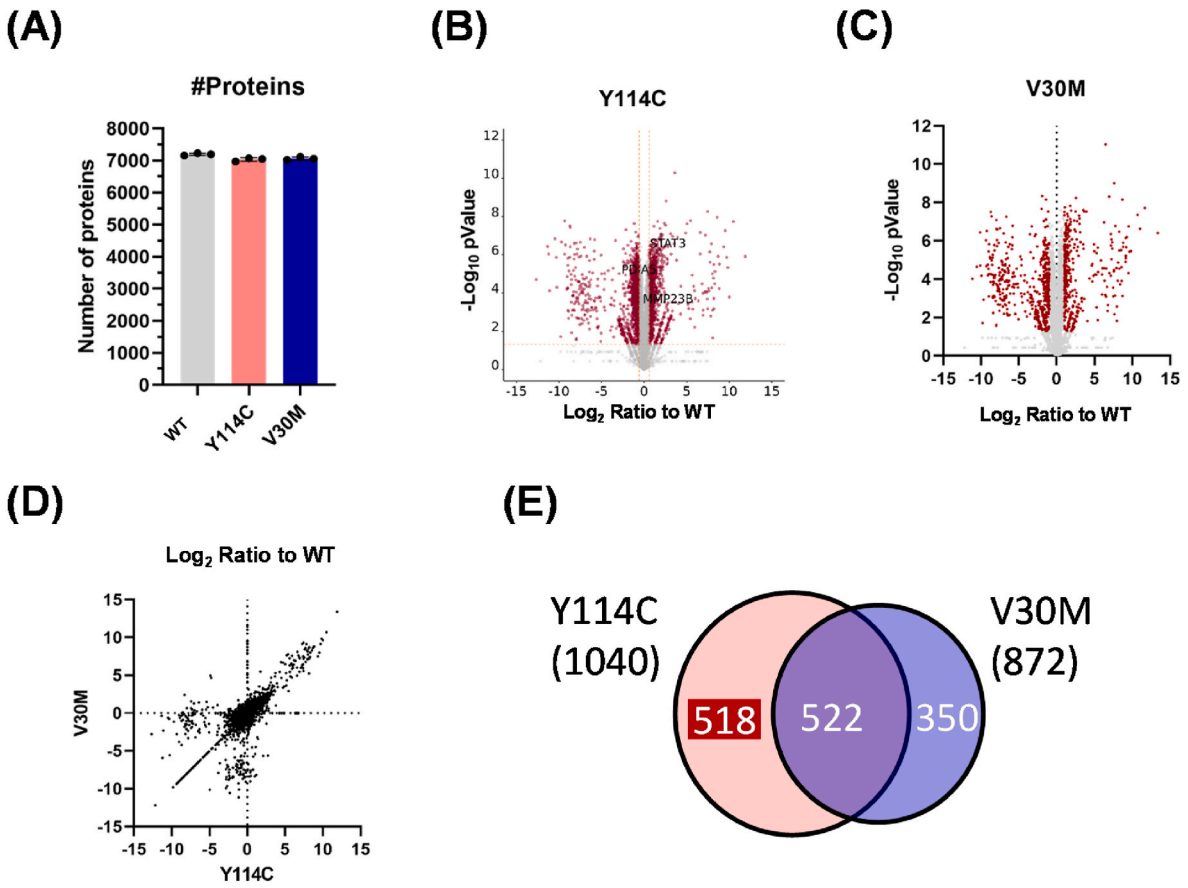

Fig. 1. Proteome analysis of HLCs (A) Protein number detected by proteome analysis was about 7194 (WT), 7030 (Y114C), and 7064 (V30 M) in HLCs, respectively. Volcano plots (red plots) showed proteins changed more than 2-folds in Y114C-HLCs (B) and V30M-HLCs (C), compared with WT-HLCs. (D, E) The number of proteins changed more than 2-folds in Y114C-HLCs and V30M-HLCs, compared with WT-HLCs.

showed the increased or decreased protein expression in Y114C-HLCs and V30M-HLCs, respectively (Fig. 1B and C). The red plot represents proteins that have significantly altered expression levels ($|\text{Log}_2 \text{ ratio}| \geq 1$ and $-\text{Log}_{10} p$ value > 1.301 (p value < 0.05)). In addition, we identified the presence of significantly altered protein expression in Y114C-HLCs and V30M-HLCs, respectively, and found the characteristic proteins in each of HLCs (Fig. 1D). There were 1040 types of proteins varied in Y114C-HLCs, and 518 proteins were changed only in Y114C-HLCs (Fig. 1E, Supplemental Table), while 350 of 870 proteins only in V30M-HLCs. Thus, we successfully identified the specific protein changed only in Y114C-HLCs, which might be involved in the specific pathogenesis of ATTR Tyr114Cys amyloidosis.

3.2. Gene ontology analysis of HLCs

Next, Gene ontology (GO) analysis was performed to further characterize the proteins significantly expressed in Y114C-HLCs. GO analysis focusing of 1040 (Fig. 2A) and 518 (Fig. 2B) specific proteins in Y114C-HLCs revealed the top 20 intracellular signals, respectively. In addition, the top 20 intracellular signals in V30M-HLCs were also identified (Fig. 2C and D). Those results suggested that the intracellular signals identified from 1040 proteins changed in Y114C-HLCs were partially overlapped with those in V30M-HLCs (Fig. 2A–C). Moreover, as expected, the intracellular signals identified from 518 proteins changed only in Y114C-HLCs were quite different from those of V30M-HLCs, such as, extracellular matrix (ECM) organization, NABA ECM regulator, cellular response to stress (Fig. 2B–D). The results of Y114C vs. V30 M comparison also confirmed the identified intracellular signals (Supplemental Fig. 1).

Gene ontology (GO) analysis by Metascape (https://metascape.org/gp/#/main/step1) showed cellular process identified by protein expression in Y114C-HLCs (A, B) and V30M-HLCs (C, D), respectively.

3.3. Reactome Pathway analysis in Y114C-HLCs

To further investigate the results of GO analysis, the identified top cell signals in Y114C-HLCs, were evaluated by Reactome Pathway analysis. In case of cell signals related to ECM organization and NABA ECM regulators, Reactome Pathway analysis suggested the involvement of intracellular signals especially related to the cellular degradation process, such as, collagen degradation (Fig. 3A). Consistent with these results, the proteins related to the cellular degradation process, especially, extracellular matrix proteases, such as MMP23B, showed higher expression in Y114C-HLCs (Fig. 3B).

In addition, if we focused on the intracellular signals related to cellular response to stress, Reactome Pathway analysis suggested the involvement of senescence-associated secretory phenotype (SASP) (Fig. 4A). As shown in Fig. 4B, the heatmaps clearly showed that, the protein expression related cellular response to stress, such as, SASP-related proteins, signal transducer and activator of transcription 3 (STAT3) and ubiquitin conjugating enzyme E2 C (UBE2C), were significantly higher in Y114C-HLCs (Fig. 4B). More importantly, of the intracellular signals related to cellular response to stress, unfolded protein response (UPR), typically initiated in response to an accumulation of misfolded proteins (such as, mutated protein) in the endoplasmic reticulum (ER), were activated in Y114C-HLCs (Fig. 4C). Further analysis also indicated the significant involvement of inositol requiring enzyme 1 α (IRE1α) signaling, one of major UPR signals, in Y114C-HLCs

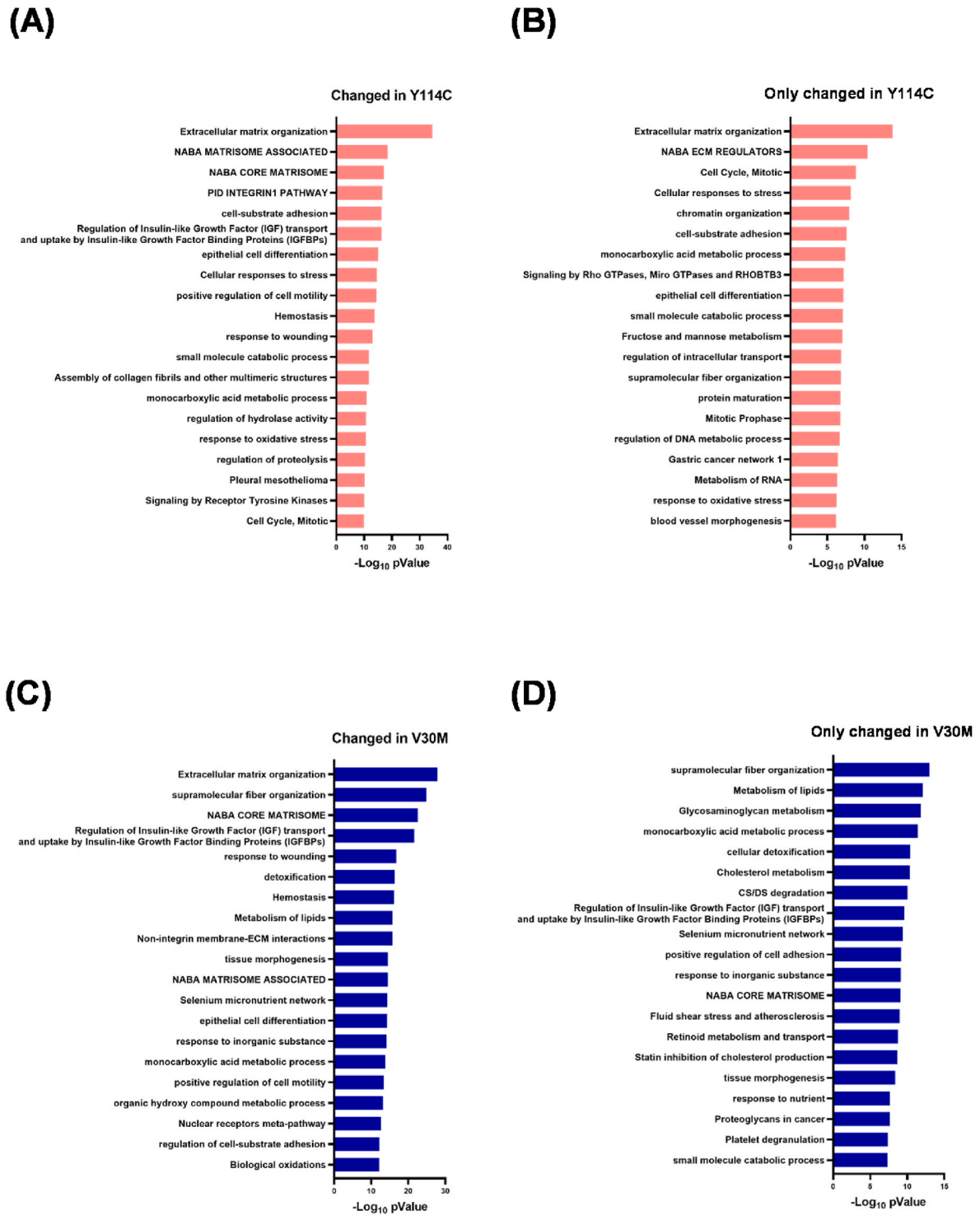

Fig. 2. GO analysis of Y114C-HLCs and V30M-HLCs.

(Fig. 4D), suggesting that the intracellular signals related to UPR might be involved in the specific pathogenesis of ATTR Tyr114Cys amyloidosis, especially focusing on TTR synthesis process.

4. Discussion

Despite the urgent need to develop novel therapy, the molecular pathogenesis of ATTR Tyr114Cys amyloidosis is still largely unknown. In this study, taking advantage of ATTRv amyloidosis-specific iPS cells and proteome analysis, we successfully identified the intracellular signals, such as, cellular response to stress and extracellular matrix organization, are activated only in Y114C-HLCs, which might be involved in the specific pathogenesis of ATTR Tyr114Cys amyloidosis, especially focusing on TTR synthesis process. In fact, ATTRv amyloidosis exhibits several different phenotypes depending on each specific TTR mutation [3]. Although proteome analysis detected approximately 7000 protein expressions in WT, Y114C and V30M-HLCs, respectively (Fig. 1A), it should be noted that more than 500 proteins expression were altered only in Y114C-HLCs (Fig. 1E). Considering the difference from V30M-HLCs and WT-HLCs, this evidence strongly suggests that the

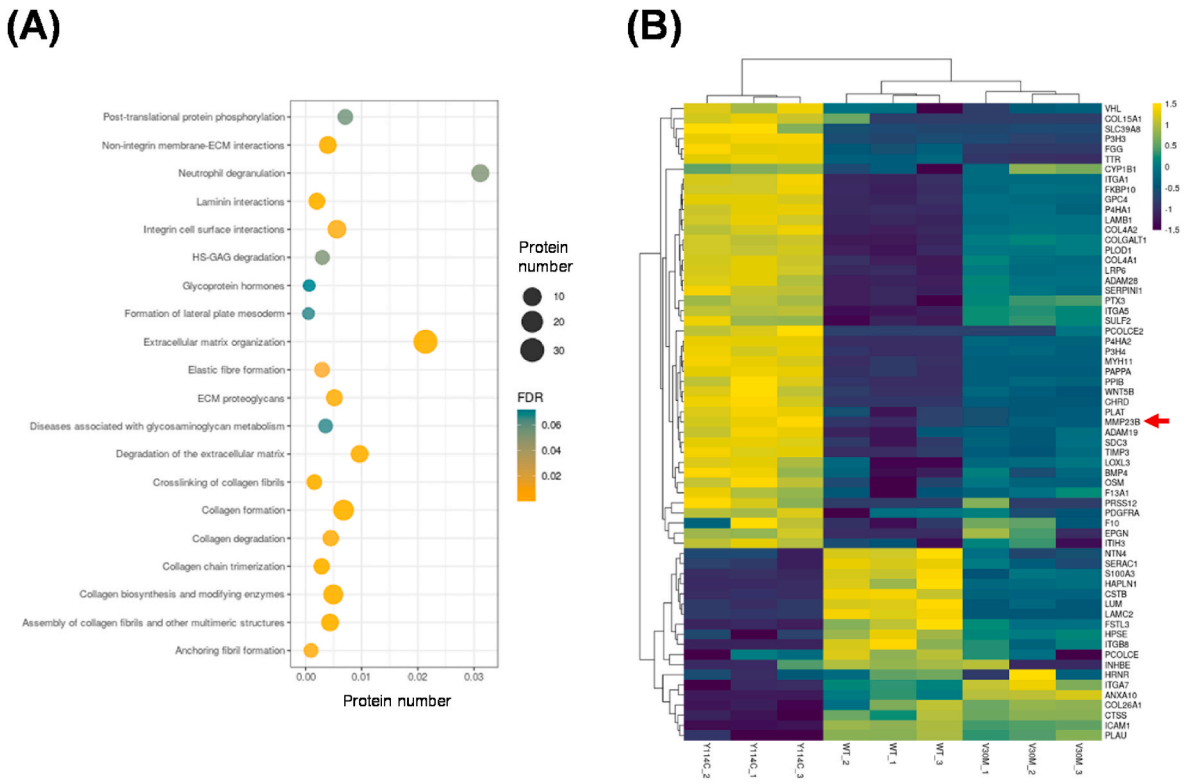

Fig. 3. Reactome Pathway analysis of extracellular matrix related signals in Y114C-HLCs (A) Reactome Pathway was performed by means of inputting identified proteins from extracellular matrix organization and NABA ECM regulator, by focusing on the proteins changed only in Y114C-HLCs by GO analysis. FDR; False discovery rate. (B) Expression patterns shown in heatmaps with identified proteins from extracellular matrix organization and NABA ECM regulator by focusing on the proteins changed only in Y114C-HLCs by GO analysis. Gene expression levels are indicated by the color bar above the heatmap (yellow, up-regulated; navy, down-regulated). MMP23B; Matrix metalloproteinase 23B.

specific point mutation (only one amino acid replacement in this case) may cause dynamic changes of cellular response. Because this kind of specific molecular analysis is difficult to be performed using clinical specimen, it also indicated the usefulness & potential of our established iPS cell lines for elucidating the molecular pathogenesis of ATTRv amyloidosis, especially in TTR producing HLCs.

In view of elucidating the specific pathogenesis, we unveiled that the intracellular signals related to UPR might be involved in the specific pathogenesis of ATTR Tyr114Cys amyloidosis (Fig. 4C and D). Our preliminary experiment indeed showed the increased expression of SULT1A3, related to IRE1α pathway in the UPR, at mRNA levels inY114C-HLCs (Supplemental Fig. 2A) [24]. It has been reported that blood ATTR-Y114C shows low concentration, unlike ATTR Val30Met amyloidosis [12]. Although our previous study revealed that Y114C-HLCs indeed secreted low ATTR-Y114C levels compared with V30M-HLCs [13,14], the molecular mechanism has been largely unknown. It is likely that the low level of ATTR-Y114C secretion from the liver is caused by UPR. Previous studies have suggested low kinetic stability TTR (such as Y114C, A25T (alanine to threonine at codon 25) and L55P (leucine to proline at codon 55), defined by TTR tetrameric dissociation rates, secrete at low levels *in vitro* [25–27]. In addition, it has been reported that secretion of unstable TTR suppressed by ATF6, major protein of UPR, such as ATTR-A25T and ATTR-L55P [28,29]. Our proteomic analysis clearly showed that IRE1α might play important roles in Y114C-HLCs (Fig. 4C and D), suggesting that low level ATTR-Y114C from the liver related in IRE1α of UPR. On the other hand, ATF6 could be unlikely involved in Y114C-HLCs, even though protein disulfide-isomerase A5 (PDIA5) identified in this study reported to be involved in ATF6 [30]. It is noted that, our preliminary phospho-proteome analysis identified protein disulfide-isomerase A6 (PDIA6) associated with UPR, in Y114C-HLCs (data not shown). PDIA6 is responsible for inhibiting excessive IRE1α signaling responses [31]. This may be a result in favor of no liver damage in patients with ATTR Tyr114Cys amyloidosis [32]. On the other hand, in contrast to ATTR-Y114C, because UPR responses were not detected in V30M-HLCs, ATTR-V30 M can be passed through UPR as WT-TTR secretion. Thus, especially focusing on TTR synthesis process, our results suggest that UPR may at least contribute to low secretion of ATTR-Y114C protein in Y114C-HLCs. Additionally, in view of involvement of SASP in the cellular response to stress, the activation of in Y114C-HLCs may support the fact that the onset of patients with ATTR Tyr114Cys is often earlier (about 40 years old ~) than that of patients with other mutations [3,5]. As shown in Fig. 3B, STAT3 and UBE2C, SASP-related proteins, were significantly higher in Y114C-HLCs, suggesting the involvement of SASP in the pathogenesis of ATTR Tyr114Cys. In view of SASP-related proteins, our preliminary experiment showed the increased expression of interleukin (IL)-8 at mRNA levels in Y114C-HLCs (Supplemental Fig. 2B). Moreover, STAT3, one of SASP-related protein, was also activated at phosphorylation levels in Y114C-HLCs (Supplemental Fig. 2C). Other study has suggested that SASP may be associated with extracellular matrix proteases [33]. The GO analysis also showed that the ECM organization and NABA ECM regulator were indeed involved in Y114C-HLCs (Fig. 3A). By taking ECM into consideration, our further analysis also found that activated ECM degradation and collagen degradation (Fig. 3B). Intriguingly, matrix metalloproteinase 9 (MMP9), one of the extracellular matrix proteases, has been reported to degrade TTR [34], and our results also showed that extracellular matrix proteases such as MMP23B, one of the MMPs, have been identified in Y114C-HLCs. MMP23B, a type II transmembrane MMP with a distinctive domain architecture and function, has an N-terminal signal anchor that targets it to the cell membrane [35]. Although some reports showed MMP23B might be involved in various cancers [36], it is first reports

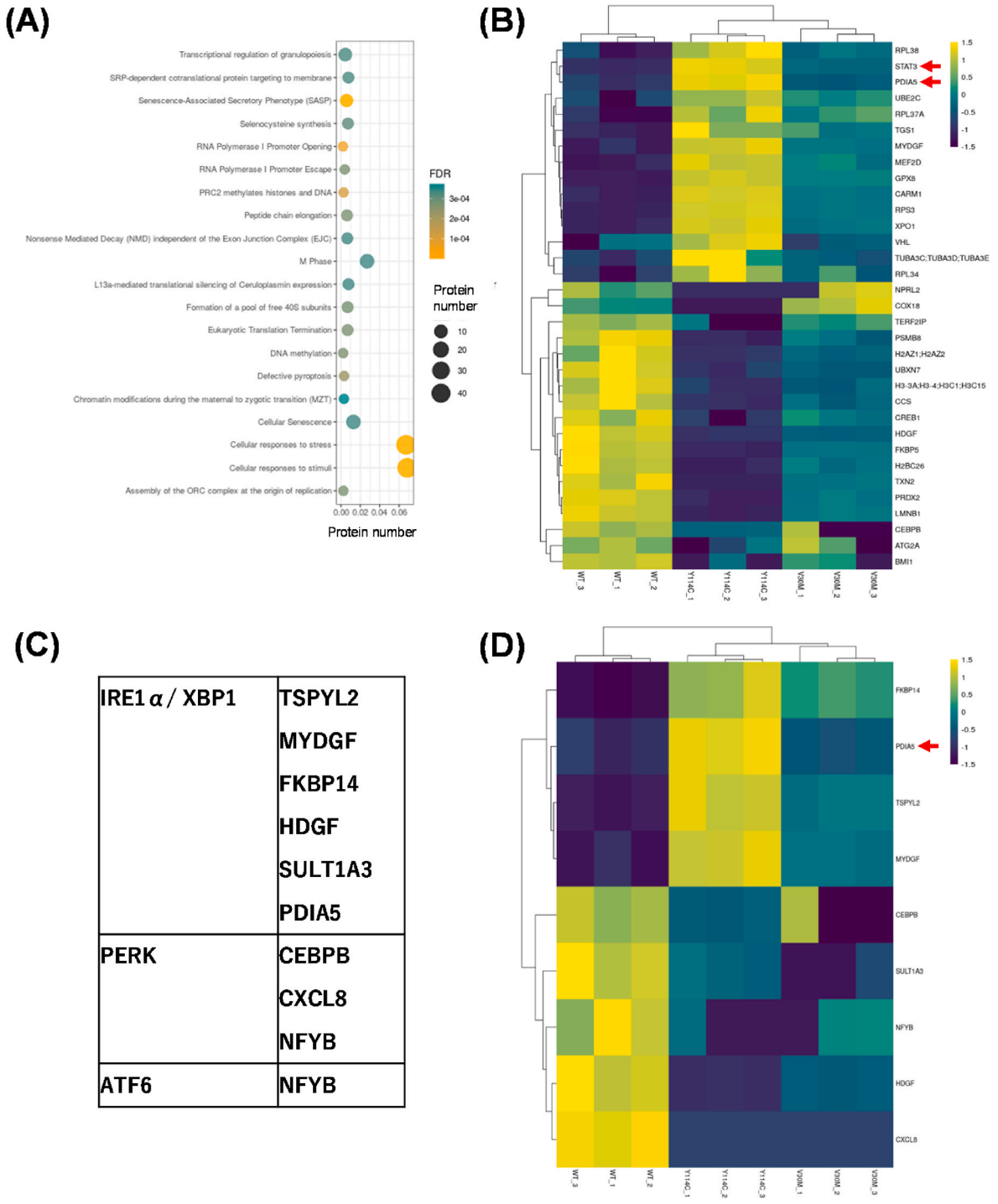

Fig. 4. Pathway analysis for cellular response to stress from GO analysis in Y114C-HLCs (A) The results of Reactome pathway analysis were shown using a dot plot. FDR; False discovery rate. (B) Expression patterns shown in heatmaps with identified as cellular response to stress proteins by focusing on the proteins changed only in Y114C-HLCs by GO analysis. Gene expression levels are indicated by the color bar above the heatmap (yellow, up-regulated; navy, down-regulated). STAT3; signal transducers and activator of transcription 3. PDIA5; protein disulfide-isomerase A5. (C) Proteins involved in UPR in Y114C-HLCs were identified using Reactome pathway analysis. (D) Expression patterns shown in heatmaps with identified proteins related to UPR by focusing on the proteins changed only in Y114C-HLCs by GO analysis. Gene expression levels are indicated by the color bar above the heatmap (yellow, up-regulated; navy, down-regulated).

suggesting the possible involvement of MMP23B in ATTR Tyr114Cys amyloidosis. Thus, the several specific intracellular signals involved in the pathogenesis of ATTR Tyr114Cys amyloidosis, need to be further investigated.

This study has limitation. Since the ATTR Tyr114Cys amyloidosis is categorized as a kind of rare disease, the number of iPS cells derived from patients is limited. In addition, it is documented that leptomeningeal-dominant type of ATTR Tyr114Cys amyloidosis exhibits various CNS symptoms, and TTR is also synthesized in the choroid plexuses of the brain. Thus, in addition to Y114C-HLCs, it is worth differentiating Y114C-iPS cells to choroid plexus cells to elucidate pathogenesis of ATTR Tyr114Cys amyloidosis in CNS symptoms in the future [37]. Furthermore, although disease-specific iPS cells may have potential to be the useful pathological models maintaining patient's

genetic information, the validation using *in vivo* models, such as ATTR Tyr114Cys transgenic mouse model, is absolutely required. Since *in vivo* models of ATTR Tyr114Cys amyloidosis have yet to be established yet, it is also necessary to establish appropriate *in vivo* models reflecting the exact symptoms of patients with ATTR Tyr114Cys amyloidosis, and validate our findings in the future.

In conclusion, our results showed that the dynamic changes of cellular response were occurred by the specific point mutation in ATTRv amyloidosis, and identified the specific intracellular signals, might be involved in the specific pathogenesis of ATTR Tyr114Cys amyloidosis.

CRediT authorship contribution statement

Kenta Ouchi: Writing – original draft, Investigation, Formal analysis, Data curation. **Takeshi Masuda:** Methodology, Formal analysis, Data curation. **Kou Yonemaru:** Investigation, Formal analysis. **Kaori Isono:** Resources. **Yuki Ohya:** Resources. **Nobuaki Shiraki:** Methodology. **Masayoshi Tasaki:** Methodology, Formal analysis, Data curation. **Yukihiro Inomata:** Supervision. **Mitsuharu Ueda:** Supervision. **Takumi Era:** Supervision, Resources, Methodology. **Shoen Kume:** Supervision. **Yukio Ando:** Supervision. **Hirofumi Jono:** Writing – review & editing, Supervision, Project administration, Investigation, Funding acquisition, Formal analysis, Data curation, Conceptualization.

Declaration of competing interest

The authors declare that they have no known competing financial interests or personal relationships that could have appeared to influence the work reported in this paper.

Acknowledgement

This research was partially supported by Research Support Project for Life Science and Drug Discovery (Basis for Supporting Innovative Drug Discovery and Life Science Research (BINDS)) from AMED under Grant Number JP23ama121018. This work was supported by Grants-in-Aid (17K19498 & 15K15006 to H.J.) from MEXT KAKENHI the Ministry of Education, Culture, Sports, Science and Technology of Japan.

Appendix A. Supplementary data

Supplementary data to this article can be found online at https://doi.org/10.1016/j.bbrep.2025.102012.

References

[1] Y. Ando, M. Nakamura, S. Araki, Transthyretin-related familial amyloidotic polyneuropathy, Arch. Neurol. 62 (2005) 1057–1062, https://doi.org/10.1001/ARCHNEUR.62.7.1057.

[2] D.C. Berry, N. Noy, Signalling by vitamin A and retinol-binding protein in regulation of insulin responses and lipid homeostasis, Biochim. Biophys. Acta Mol. Cell Biol. Lipids 1821 (2012) 168–176, https://doi.org/10.1016/j.bbalip.2011.07.002.

[3] T. Yamashita, M. Ueda, Y. Misumi, T. Masuda, T. Nomura, M. Tasaki, K. Takamatsu, K. Sasada, K. Obayashi, H. Matsui, Y. Ando, Genetic and clinical characteristics of hereditary transthyretin amyloidosis in endemic and non-endemic areas: experience from a single-referral center in Japan, J. Neurol. 265 (2018) 134–140, https://doi.org/10.1007/S00415-017-8640-7/FIGURES/6.

[4] Y. Ando, M.D.R. Almeida, P.I. Ohlsson, E. Ando, A. Negi, O. Suhr, H. Terazaki, K. Obayashi, M. Ando, M.J.M. Saraiva, Unusual self-association properties of transthyretin Y114C related to familial amyloidotic polyneuropathy: effects on detection and quantification, Biochem. Biophys. Res. Commun. 261 (1999) 264–269, https://doi.org/10.1006/BBRC.1999.1048.

[5] M. Nakamura, T. Yamashita, M. Ueda, K. Obayashi, T. Sato, T. Ikeda, Y. Washimi, T. Hirai, Y. Kuwahara, M.T. Yamamoto, M. Uchino, Y. Ando, Neuroradiologic and clinicopathologic features of oculoleptomeningeal type amyloidosis, Neurology 65 (2005) 1051–1056, https://doi.org/10.1212/01.WNL.0000178983.20975.AF.

[6] T. Coelho, L.F. Maia, A.M. Da Silva, M.W. Cruz, V. Planté-Bordeneuve, O.B. Suhr, I. Conceiçao, H.H.J. Schmidt, P. Trigo, J.W. Kelly, R. Labaudinière, J. Chan, J. Packman, D.R. Grogan, Long-term effects of tafamidis for the treatment of transthyretin familial amyloid polyneuropathy, J. Neurol. 260 (2013) 2802, https://doi.org/10.1007/S00415-013-7051-7.

[7] D. Adams, A. Gonzalez-Duarte, W.D. O'Riordan, C.-C. Yang, M. Ueda, A.V. Kristen, I. Tournev, H.H. Schmidt, T. Coelho, J.L. Berk, K.-P. Lin, G. Vita, S. Attarian, V. Planté-Bordeneuve, M.M. Mezei, J.M. Campistol, J. Buades, T.H. Brannagan, B. J. Kim, J. Oh, Y. Parman, Y. Sekijima, P.N. Hawkins, S.D. Solomon, M. Polydefkis, P.J. Dyck, P.J. Gandhi, S. Goyal, J. Chen, A.L. Strahs, S.V. Nochur, M.T. Sweetser, P.P. Garg, A.K. Vaishnaw, J.A. Gollob, O.B. Suhr, Patisiran, an RNAi therapeutic, for hereditary transthyretin amyloidosis, N. Engl. J. Med. 379 (2018) 11–21, https://doi.org/10.1056/NEJMOA1716153/SUPPL_FILE/NEJMOA1716153_DISCLOSURES.PDF.

[8] G. Holmgren, L. Steen, O. Suhr, B.G. Ericzon, C.G. Groth, O. Andersen, B.G. Wallin, A. Seymour, S. Richardson, P.N. Hawkins, M.B. Pepys, Clinical improvement and amyloid regression after liver transplantation in hereditary transthyretin amyloidosis, Lancet 341 (1993) 1113–1116, https://doi.org/10.1016/0140-6736(93)93127-M.

[9] K. Takahashi, S. Yamanaka, Induction of pluripotent stem cells from mouse embryonic and adult fibroblast cultures by defined factors, Cell 126 (2006) 663–676, https://doi.org/10.1016/J.CELL.2006.07.024.

[10] K. Takahashi, K. Tanabe, M. Ohnuki, M. Narita, T. Ichisaka, K. Tomoda, S. Yamanaka, Induction of pluripotent stem cells from adult human fibroblasts by defined factors, Cell 131 (2007) 861–872, https://doi.org/10.1016/J.CELL.2007.11.019.

[11] J. Yu, M.A. Vodyanik, K. Smuga-Otto, J. Antosiewicz-Bourget, J.L. Frane, S. Tian, J. Nie, G.A. Jonsdottir, V. Ruotti, R. Stewart, I.I. Slukvin, J.A. Thomson, Induced pluripotent stem cell lines derived from human somatic cells, Science (1979) 318 (2007) 1917–1920, https://doi.org/10.1126/SCIENCE.1151526/SUPPL_FILE/YU.SOM.REVISION.1.PDF.

[12] M. Ueda, Y. Misumi, M. Mizuguchi, M. Nakamura, T. Yamashita, Y. Sekijima, K. Ota, S. Shinriki, H. Jono, S.I. Ikeda, O.B. Suhr, Y. Ando, SELDI-TOF mass spectrometry evaluation of variant transthyretins for diagnosis and pathogenesis of familial amyloidotic polyneuropathy, Clin. Chem. 55 (2009) 1223–1227, https://doi.org/10.1373/CLINCHEM.2008.118505.

[13] K. Ouchi, K. Isono, Y. Ohya, N. Shiraki, M. Tasaki, Y. Inomata, M. Ueda, T. Era, S. Kume, Y. Ando, H. Jono, Characterization of heterozygous ATTR Tyr114Cys amyloidosis-specific induced pluripotent stem cells, Heliyon 10 (2024) e24590, https://doi.org/10.1016/J.HELIYON.2024.E24590.

[14] K. Isono, H. Jono, Y. Ohya, N. Shiraki, T. Yamazoe, A. Sugasaki, T. Era, N. Fusaki, M. Tasaki, M. Ueda, S. Shinriki, Y. Inomata, S. Kume, Y. Ando, Generation of familial amyloidotic polyneuropathy-specific induced pluripotent stem cells, Stem Cell Res. 12 (2014) 574–583, https://doi.org/10.1016/j.scr.2014.01.004.

[15] T. Masuda, N. Saito, M. Tomita, Y. Ishihama, Unbiased quantitation of Escherichia coli membrane proteome using phase transfer surfactants, Mol. Cell. Proteomics 8 (2009) 2770, https://doi.org/10.1074/MCP.M900240-MCP200.

[16] T. Masuda, M. Tomita, Y. Ishihama, Phase transfer surfactant-aided trypsin digestion for membrane proteome analysis, J. Proteome Res. 7 (2008) 731–740, https://doi.org/10.1021/PR700658Q/SUPPL_FILE/PR700658Q-FILE007.PDF.

[17] J. Rappsilber, Y. Ishihama, M. Mann, Stop and go extraction tips for matrix-assisted laser desorption/ionization, nanoelectrospray, and LC/MS sample pretreatment in proteomics, Anal. Chem. 75 (2003) 663–670, https://doi.org/10.1021/AC026117I.

[18] J. Rappsilber, M. Mann, Y. Ishihama, Protocol for micro-purification, enrichment, pre-fractionation and storage of peptides for proteomics using StageTips, Nat. Protoc. 2 (2007) 1896–1906, https://doi.org/10.1038/nprot.2007.261.

[19] V. Demichev, C.B. Messner, S.I. Vernardis, K.S. Lilley, M. Ralser, DIA-NN: neural networks and interference correction enable deep proteome coverage in high throughput, Nat. Methods 17 (2020) 41–44, https://doi.org/10.1038/s41592-019-0638-x, 2019.

[20] J. Cox, M. Mann, MaxQuant enables high peptide identification rates, individualized p.p.b.-range mass accuracies and proteome-wide protein quantification, Nat. Biotechnol. 26 (2008) 1367–1372, https://doi.org/10.1038/nbt.1511.

[21] S. Okuda, Y. Watanabe, Y. Moriya, S. Kawano, T. Yamamoto, M. Matsumoto, T. Takami, D. Kobayashi, N. Araki, A.C. Yoshizawa, T. Tabata, N. Sugiyama, S. Goto, Y. Ishihama, jPOSTrepo: an international standard data repository for proteomes, Nucleic Acids Res. 45 (2017) D1107–D1111, https://doi.org/10.1093/NAR/GKW1080.

[22] Y. Zhou, B. Zhou, L. Pache, M. Chang, A.H. Khodabakhshi, O. Tanaseichuk, C. Benner, S.K. Chanda, Metascape provides a biologist-oriented resource for the analysis of systems-level datasets, Nat. Commun. 10 (2019) 1523, https://doi.org/10.1038/S41467-019-09234-6.

[23] D. Croft, A.F. Mundo, R. Haw, M. Milacic, J. Weiser, G. Wu, M. Caudy, P. Garapati, M. Gillespie, M.R. Kamdar, B. Jassal, S. Jupe, L. Matthews, B. May, S. Palatnik, K. Rothfels, V. Shamovsky, H. Song, M. Williams, E. Birney, H. Hermjakob, L. Stein, P. D'Eustachio, The Reactome pathway knowledgebase, Nucleic Acids Res. 42 (2014) D472–D477, https://doi.org/10.1093/NAR/GKT1102.

[24] C. Kakiuchi, M. Ishiwata, A. Hayashi, T. Kato, XBP1 induces WFS1 through an endoplasmic reticulum stress response element-like motif in SH-SY5Y cells, J. Neurochem. 97 (2006) 545–555, https://doi.org/10.1111/J.1471-4159.2006.03772.X.

[25] Y. Sekijima, R.L. Wiseman, J. Matteson, P. Hammarström, S.R. Miller, A.R. Sawkar, W.E. Balch, J.W. Kelly, The biological and chemical basis for tissue-selective amyloid disease, Cell 121 (2005) 73–85, https://doi.org/10.1016/J.CELL.2005.01.018.

[26] R.B. Ibrahim, S.Y. Yeh, K.P. Lin, F. Ricardo, T.Y. Yu, C.C. Chan, J.W. Tsai, Y.T. Liu, Cellular secretion and cytotoxicity of transthyretin mutant proteins underlie late-onset amyloidosis and neurodegeneration, Cell. Mol. Life Sci. 77 (2020) 1421–1434, https://doi.org/10.1007/s00018-019-03357-1.

[27] T. Sato, S. Susuki, M.A. Suico, M. Miyata, Y. Ando, M. Mizuguchi, M. Takeuchi, M. Dobashi, T. Shuto, H. Kai, Endoplasmic reticulum quality control regulates the fate of transthyretin variants in the cell, EMBO J. 26 (2007) 2501–2512, https://doi.org/10.1038/SJ.EMBOJ.7601685.

[28] J.J. Chen, J.C. Genereux, S. Qu, J.D. Hulleman, M.D. Shoulders, R.L. Wiseman, ATF6 activation reduces the secretion and extracellular aggregation of destabilized variants of an amyloidogenic protein, Chem Biol 21 (2014) 1564–1574, https://doi.org/10.1016/J.CHEMBIOL.2014.09.009.

[29] R.M. Giadone, D.C. Liberti, T.M. Matte, J.D. Rosarda, C. Torres-Arancivia, S. Ghosh, J.K. Diedrich, S. Pankow, N. Skvir, J.C. Jean, J.R. Yates, A.A. Wilson, L. H. Connors, D.N. Kotton, R.L. Wiseman, G.J. Murphy, Expression of amyloidogenic transthyretin drives hepatic proteostasis remodeling in an induced pluripotent stem cell model of systemic amyloid disease, Stem Cell Rep. 15 (2020) 515–528, https://doi.org/10.1016/j.stemcr.2020.07.003.

[30] A. Higa, S. Taouji, S. Lhomond, D. Jensen, M.E. Fernandez-Zapico, J.C. Simpson, J.-M. Pasquet, R. Schekman, E. Chevet, Endoplasmic reticulum stress-activated transcription factor ATF6α requires the disulfide isomerase PDIA5 to modulate chemoresistance, Mol. Cell Biol. 34 (2014) 1839–1849, https://doi.org/10.1128/MCB.01484-13.

[31] D. Eletto, D. Eletto, D. Dersh, T. Gidalevitz, Y. Argon, Protein disulfide isomerase A6 controls the decay of IRE1α signaling via disulfide-dependent association, Mol Cell 53 (2014) 562–576, https://doi.org/10.1016/J.MOLCEL.2014.01.004.

[32] A.J. Stangou, N.D. Heaton, M. Rela, M.B. Pepys, P.N. Hawkins, R. Williams, Domino hepatic transplantation using the liver from a patient with familial amyloid polyneuropathy, Transplantation 65 (1998) 1496–1498, https://doi.org/10.1097/00007890-199806150-00016.

[33] Y.A. Mebratu, S. Soni, L. Rosas, M. Rojas, J.C. Horowitz, R. Nho, The aged extracellular matrix and the profibrotic role of senescence-associated secretory phenotype, Am J Physiol Cell Physiol 325 (2023) C565–C579, https://doi.org/10.1152/AJPCELL.00124.2023/ASSET/IMAGES/MEDIUM/C-00124-2023R01.PNG.

[34] I. Cardoso, M. Brito, M.J. Saraiva, Extracellular matrix markers for disease progression and follow-up of therapies in familial amyloid polyneuropathy V30M TTR-related, Dis. Markers 25 (2008) 37–47, https://doi.org/10.1155/2008/549872.

[35] G.W. Huntley, Synaptic circuit remodelling by matrix metalloproteinases in health and disease, Nat. Rev. Neurosci. 13 (2012) 743–757, https://doi.org/10.1038/NRN3320.

[36] N. Li, H. Li, L. Wei, H. Chen, Z. Wu, S. Yuwen, S. Yang, The downregulation of MMP23B facilitates the suppression of vitality and induction of apoptosis in endometrial cancer cells, Reprod. Sci. 31 (2024) 3452–3461, https://doi.org/10.1007/S43032-024-01581-0/FIGURES/5.

[37] L. Pellegrini, C. Bonfio, J. Chadwick, F. Begum, M. Skehel, M.A. Lancaster, Human CNS barrier-forming organoids with cerebrospinal fluid production, Science (1979) (2020) 369, https://doi.org/10.1126/SCIENCE.AAZ5626/SUPPL_FILE/AAZ5626_PELLEGRINI_SM_REV1.PDF.